



Foaming, emulsifying and rheological properties of extracts from a co-product of the Quorn fermentation process

Julien Lonchamp¹ · P. S. Clegg² · S. R. Euston³

Received: 22 January 2019 / Revised: 10 April 2019 / Accepted: 27 April 2019 / Published online: 24 May 2019
© The Author(s) 2019

Abstract

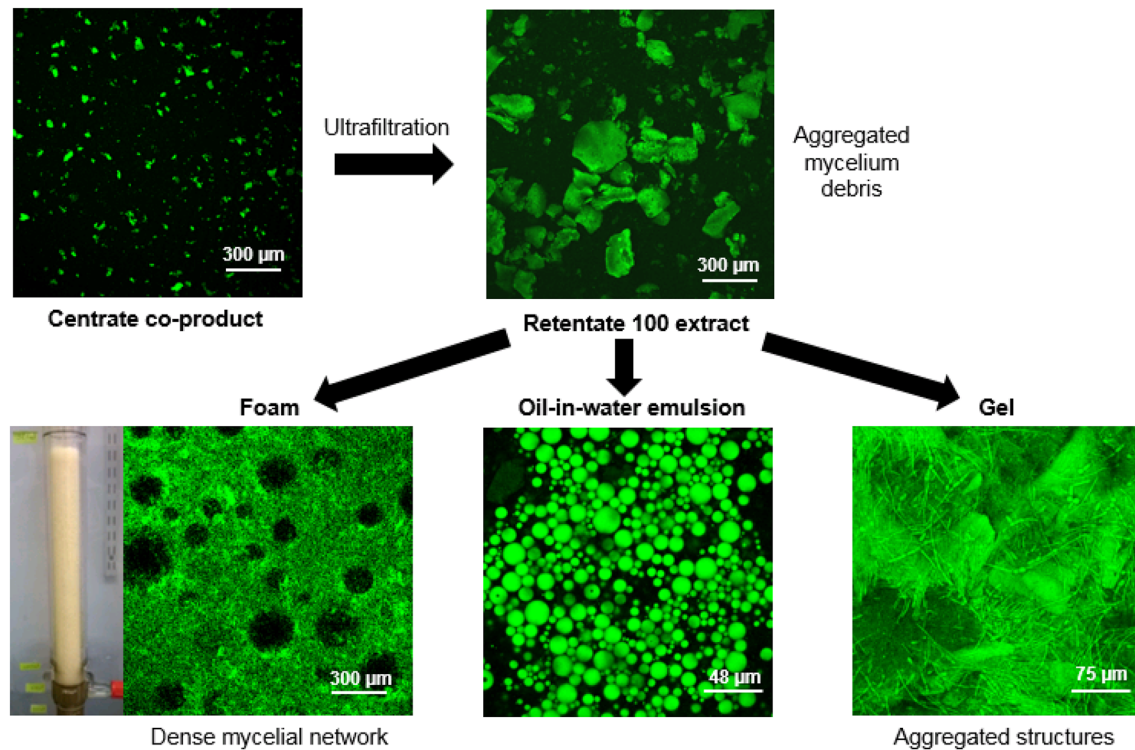
This study assessed the functional profile (foaming, emulsifying and rheological properties), proteomic and metabolomic composition of a naturally foaming and currently unexploited co-product (centrate) from the Quorn fermentation process. Due to the low environmental footprint of this process the centrate is a potential source of sustainable functional ingredients for the food industry. A range of fractions were isolated from the centrate via successive ultrafiltration steps. The retentate 100 (R100) fraction, which was obtained following a 100 kDa ultrafiltration, displayed good foaming, emulsifying and rheological properties. R100 solutions and oil-in-water emulsions displayed high viscosity, while R100 solutions and hydrogels showed high viscoelasticity. R100 foams displayed high stability while oil-in-water R100 emulsions showed small and stable oil droplet size distributions. Large mycelial aggregates were reported in R100 solutions and gels, correlating with their high viscosity and viscoelasticity. A dense mycelial network was observed in R100 foams and contributing to their stability. In parallel tensiometry measurements highlighted the presence of interfacially active molecules in R100 which formed a rigid film stabilising the oil/water interface. A number of functional metabolites and proteins were identified in the centrate, including a cerato-platanin protein, cell membrane constituents (phospholipids, sterols, glycosphingolipids, sphingomyelins), cell wall constituents (chitin, chitosan, proteins), guanine and guanine-based nucleosides and nucleotides. This study highlighted the potential of functional extracts from the Quorn fermentation process as novel ingredients for the preparation of sustainable food products and the complex and specific nature of the centrate's functional profile, with contributions reported for both mycelial structures and interfacially active molecules.

Electronic supplementary material The online version of this article (<https://doi.org/10.1007/s00217-019-03287-z>) contains supplementary material, which is available to authorized users.

✉ Julien Lonchamp
JLonchamp@qmu.ac.uk

- ¹ Present Address: School of Health Sciences, Queen Margaret University, Queen Margaret University Drive, Edinburgh EH21 6UU, UK
- ² School of Physics and Astronomy, The University of Edinburgh, Peter Guthrie Tait Road, Edinburgh EH9 3FD, UK
- ³ Institute of Mechanical Process and Energy Engineering, School of Engineering and Physical Sciences, Heriot-Watt University, Edinburgh EH14 4AS, UK

Graphical abstract



Keywords Quorn · Co-product · Centrate · Rheology · Foam · Emulsion

Introduction

Animal-derived functional ingredients including milk and egg proteins play a key role in the food industry due to their ability to form gels and to stabilise oil droplets in emulsions and air bubbles in foams. However, due to their high environmental costs and market volatility, the food industry is looking for sustainable alternatives [1]. One of the strategies employed consists in screening unexploited co-product streams from the food industry for extraction of potential functional alternatives. In this context the production of fungal proteins by Marlow Foods for use in their meat alternative product Quorn is a potential source of sustainable functional ingredients. The term mycoprotein refers to the high-protein biomass produced by fermentation of the fungus *Fusarium venenatum* A3/5 (ATCC PTA-2684) by Marlow Foods, which forms the basis of their Quorn brand products. Mycoprotein contains all essential amino acids [2] and the net protein utilisation value of *Fusarium venenatum* mycoprotein is comparable to that of milk [3]. Moreover, the fermentation of starch into protein by *F. venenatum* results in 90% lower emission of greenhouse gases and benefits in terms of land and water footprints in comparison with beef products [4].

Currently mycoprotein biomass is marketed as the meat substitute Quorn. However, a liquid co-product stream that contains residual hyphal biomass, carbohydrates, nucleotides and proteins as well as the residues of the fermentation feedstock is produced as part of the fermentation process and is currently unexploited. This co-product (centrate) is generated as a result of an RNA-reduction step in which the fermentation broth is first heat-shocked above 68 °C for 30–45 min, then further heated at 90 °C and finally centrifuged [5]. The resulting solid deposit (mycoprotein biomass) is processed into a dough ready for conversion to the meat-like texture characteristic of Quorn foods, while centrate is the liquid centrifugation supernatant. This heat shock step carried out on the fermentation broth stops growth, disrupts ribosomes and activates endogenous RNAases which break down cellular RNA to nucleotides [5]. Heat shock also induces diffusion of a fraction of the cell components through the cell wall, including nucleotides and proteinaceous material [5]. The resulting presence of these cell components in the centrate leads to foaming in the centrifuge, indicating the presence of surface-active material.

With only 49 proteins listed on Uniprot (Universal Protein Resource), the *Fusarium venenatum* proteome has so far not been fully characterised [6]. Several protein families

produced by filamentous fungi have been reported to be surface-active, including hydrophobins, repellents, rodlinins, chaplins, SapB, fungispumins and cerato-platanins [7–9]. One hydrophobin and eight proteins of the cerato-platanin family were reported on Uniprot for *Gibberella zeae* (*Fusarium graminearum* or wheat head blight fungus) [6], which belongs to the same *Fusarium sambucinum* species complex as *Fusarium venenatum*. Filamentous fungi secrete cerato-platanin proteins (CPPs) extracellularly into the culture filtrate, but they have been also reported within the cell wall of fungal hyphae and spores [10, 11]. Frischmann et al. [9] reported that the cerato-platanin EPL1 from *Trichoderma atroviride* self-assembles into regularly patterned protein biofilms at air/water interfaces and that EPL1 protein solutions exhibited strong foaming properties.

Denny et al. [2] reported a 6% dietary fibre content for mycoprotein biomass with a predominance of the fungal cell-wall components beta-glucans and *N*-acetylglucosamine polymers (chitin and chitosan). Beta-glucan extracts from barley and oats are used as functional ingredients in the food industry due to their thickening, emulsifying, water-holding capacity, texturising, stabilising, and gelling properties [12]. Similarly chitin, chitosan and their derivatives are used as functional ingredients in the food industry due to their texture-controlling, emulsifying, thickening, gelling and stabilising properties [13], including those of fungal origin [14]. Nucleotides were reported as breakdown products of RNA during the RNA-reducing heat-shock step [5]. Viscosifying and gelling properties have been reported for guanine-based nucleotides due to the ability of the nucleobase guanine to self-associate [15]. The aim of this study was to assess the proteomic and metabolomic composition of the centrate and the functional profile (foaming, emulsifying and rheological properties) of various fractions derived from the centrate to act as a benchmark for the assessment of the exploitation potential of the co-product stream.

Materials and methods

Sample preparation

Centrate samples were collected and frozen. Following thawing the centrate underwent a series of ultrafiltration steps using a range of Vivaflow 200 crossflow cassettes (Sartorius, UK) connected to a Masterflex Easy-Load peristaltic pump (Sartorius, UK). Following an initial 100 kDa ultrafiltration, the resulting retentate 100 or R100 (composed of molecules larger than 100 kDa) was collected, while the filtrate 100 underwent further ultrafiltration, using either a 5 kDa membrane or a 50 kDa followed by a 5 kDa membrane. Samples of the centrate and resulting retentates were freeze-dried in a Super Modulyo unit (Edwards, UK).

Nitrogen content

As a wide range of surface-active molecules potentially present in the centrate fractions contain nitrogen (including fungal cell membrane and cell wall constituents such as phospholipids, glycosphingolipids, sphingomyelins, chitin, chitosan and glycoproteins) the Kjeldahl method [16] was used to provide a guideline for preparation of standardised sample quantities for functional tests. 0.1 g of each powder was digested in concentrated sulphuric acid (92%) using a Kjeltec Basic Digestion Unit 20 (Foss, UK) at 440 °C in the presence of a selenium catalyst. Distillation of the digested samples into boric acid was carried out using a Tecator Kjeltec 8100 Manual Distillation Unit (Foss, UK). The distilled samples were then titrated using 0.1 N hydrochloric acid. The % nitrogen was calculated using the following formula:

$$\text{Nitrogen} = \frac{\text{titration volume (ml)} \times 14.007}{\text{sample weight (g)} \times 100}.$$

The % nitrogen obtained was then multiplied by a general conversion factor of 6.25. Measurements were repeated three times.

Gel electrophoresis

Sodium dodecyl sulphate polyacrylamide gel electrophoresis (SDS-PAGE) and native PAGE were performed on the centrate fractions using a Mini-Protean Tetra Cell System with TGX 4–20% Tris–glycine gels (Bio-Rad Laboratories Ltd., UK). 1% w/w nitrogen-containing material (NCM) solutions of the centrate fractions were prepared in deionised water and stirred for one hour.

SDS-PAGE samples were prepared by mixing equal proportions of solution and Laemmli 2× concentrate sample buffer (Sigma Aldrich Ltd., UK) followed by heating at 70 °C for 10 min. Native PAGE samples were prepared by mixing the solution with Novex native TrisGly 2× sample buffer (Life Technologies, UK) in equal proportions. A See Blue Plus2 pre-Stained standard (Life Technologies Ltd., UK) was used as molecular weight marker. The gels were run in Tris/Glycine/SDS buffer (Bio-Rad Laboratories Ltd., UK) at 100 V for 1 h and subsequently stained in a Coomassie brilliant blue solution (VWR Ltd., UK) and destained in glacial acetic acid/methanol/deionised water 1/4/5. Gels were scanned using a ChemiDoc XRS+ imaging system (Bio-Rad Laboratories Ltd., UK) and analysed using the associated Image Lab software.

Proteomics

Protein digestion was carried out according to Le Bihan et al. [17]. Samples were denatured in 8 M urea, reduced by incubation with dithiothreitol prior to cysteine alkylation with

iodoacetamide and overnight digestion with 60 µg trypsin. Four micrograms of peptide samples were acidified with 1% formic acid before centrifugation and vacuum-drying. The samples were analysed by capillary HPLC–MS/MS, using 140-min gradients as described by Martin et al. [18] on a hybrid LTQ–Orbitrap XL instrument (Thermo-Fisher, UK). HPLC quality acetonitrile (Fisher, UK), Suprapure formic acid and sequencing grade trifluoroacetic acid (Merck, Germany) were used. Multicharged (2+, 3+ and 4+) ion intensities were extracted from the LC–MS files and the Mascot Version 2.4 software (Matrix Science Ltd, UK) was used to compare the MS/MS data against the NCBI protein database with the following search parameters: maximum missed-cut value of 2, variable oxidation, N-terminal protein acetylation and fixed carbamidomethylation, precursor mass tolerance of 7 ppm and MS/MS tolerance of 0.4 Da. A significance threshold of less than 0.05 and a minimum peptide cut-off score of 20 were set. Proteins which were identified based on the *Fusarium graminearum* proteome and quantified with 2 or more peptide sequences were retained.

Metabolomics

Alcohol insoluble residues of the centrate were produced in 10 ml 70% ethanol. The vials were left overnight at room temperature and the residues were subsequently washed three times with 10 ml of a 10/10/3 chloroform/methanol/water solution by centrifugation at 2700×g for 10 min. The wash step supernatants were pooled and run in positive (pos) and negative (neg) ion mode on an 6560 Agilent Quadrupole Time of Flight (IM-QTOF) mass spectrometer (MS) (Agilent, UK). Samples were run in both ion mobility QTOF mode and MS/MS QTOF mode. A 100 mm×2.1 mm, 1.8 µm ACE C18-PFP column was used. Two solvents were used in separation (solvent A: 50% methanol, solvent B: 95% acetonitrile) using gradient elution at a flow rate of 0.2 ml/min (0 min: 10% B, 5 min: 30% B, 10–12 min: 95% B, 15–16 min: 10% B). The data were analysed using Mass Profiler (MP) and were also extracted using Profinder before uploading to Mass Profiler Professional (MPP) to carry out clustering analysis and visualise feature abundance. Alignment of samples with the Metlin accurate mass metabolite database was carried out with accurate mass matching to 10 ppm.

Rheological properties

Rheological measurements of centrate fraction solutions and oil-in-water emulsions were performed using a Bohlin Gemini controlled stress rheometer (Malvern Instruments, UK) using cone-and-plate geometry. Measurements were repeated three times.

For viscosity measurements 10% w/w NCM solutions of the centrate fractions were prepared in deionised water and stirred for 2 h. The commercial whey protein concentrate product Lacprodan 87 (L87, Arla, Denmark) was used as control for all functionality tests. The L87 solution was prepared at a higher protein concentration (15.3%) to match the solid content of a 10% NCM R100 solution (17.65% solids) and assess the possible influence of solid content on viscosity. To prepare emulsions for rheology, 15 g solutions of 5% w/w NCM centrate fractions were mixed with 5 g of sunflower oil and homogenised using an Ultra-Turrax high speed homogeniser (IKA-Werke GmbH, Germany) for 1 min. Viscosity measurements were performed using a 4°/40 mm cone (gap 150 µm) at 20 °C. The instantaneous viscosity (Pa s) was measured through a shear rate sweep test ranging from 10^{−3} to 50 s^{−1} in up-down mode (15-min up-sweep, 15-min down-sweep).

For gelation tests preliminary oscillatory measurements of elastic and viscous moduli (G' and G'') were carried out on 10% w/w NCM centrate fraction solutions at 1 Hz over a strain amplitude sweep test ranging from 0.00005 to 50 to determine the linear viscoelastic region of each sample. Small-amplitude oscillatory measurements were then performed using a 2°/40 mm cone (gap 70 µm). G' and G'' were measured through a temperature sweep test ranging from 40 to 90 °C in up-down mode (15-min up-sweep, 15-min down-sweep). The applied strain was chosen from within the linear viscoelastic region for each sample and the oscillation frequency was 1 Hz.

Foaming properties

Two types of foaming methods (gas-sparging and frothing) were carried out. The stability of foams produced by the centrate fraction solutions was first assessed using a gas-sparging test according to Rudin [19] with minor modifications. 40 g solutions of 1% w/w NCM centrate fractions were stirred for 1 h. Gas-sparging was carried out at constant flow rate of CO₂ (100 cm³/min) until the foam reached the top indicator of the column. The foam stability was quantified as the time needed for the foam to collapse to the second indicator at the bottom of the column. Measurements were repeated three times.

For frothing tests 15 g solutions of 1% w/w NCM centrate fractions were prepared in 50 ml glass beakers. The solutions were frothed for 1 min using a handheld whisk-type frother (Aerolatte, UK). The height of the resulting foam was measured with a ruler immediately after whisking and every 10 min until collapse of the foam. The foaming ability was determined as the initial height of the foam, while the foam stability was expressed as the time needed for the foam to fully collapse. Measurements were repeated twice.

Emulsifying properties

Both the EAI/ESI test and oil droplet size distribution were carried out to characterise the oil-in-water emulsions prepared with the different samples. Emulsifying activity index (EAI) and emulsion stability index (ESI) were determined according to Ogunwolu et al. [20] with some modifications. 22.5 g solutions of 1% w/w NCM centrate fractions were mixed with 7.5 g of sunflower oil (to obtain a 3:1 phase ratio) and the mixture was high-speed homogenised for 1 min to produce oil-in-water emulsions. 50 µl of the emulsion were pipetted from the bottom of the vial and suspended in 5 ml of 0.1% (w/v) SDS solution. This step was carried out immediately after emulsification then after 10 min. Absorbance of the diluted emulsions was measured at 500 nm using a Genesys 6 UV/Vis spectrophotometer (Thermo Electron Corporation, USA). The ability of the protein to form an emulsion (emulsifying activity index, EAI) and the emulsion stability index (ESI) were calculated using the following formulae:

$$\text{EAI (m}^2/\text{g)} = \frac{2 \times T \times A_0 \times \text{dilution factor}}{C \times \varnothing \times 1000}, \quad \text{ESI (min)} = \frac{A_0}{A_0 - A_{10}} \times \Delta t,$$

where $T = 2.303$, A_0 = apparent absorbance at 0 min, dilution factor = 100, C = weight per unit volume (g/ml), \varnothing = oil volumetric fraction (0.25), A_{10} = apparent absorbance after 10 min, $\Delta t = 10$ min. Measurements were repeated three times.

The average oil droplet size distribution of the centrate fraction emulsions [D (3.2) or surface weighted mean] were measured using a Mastersizer 2000 (Malvern Instruments Ltd., UK). The refractive index of oil droplets was set at 1.474 (corresponding to sunflower oil). The laser obscuration was adjusted to 10% obscuration and triplicate measurements were carried out.

Tensiometry

Both surface tension and oil/water interfacial tension were determined for the different samples. For surface tension measurements 1% w/w NCM centrate fraction solutions were serially diluted to obtain 0.5%, 0.25%, and 0.1% w/w NCM solutions. The surface tension of the solutions was measured using the Du Nouy method with an EZ-Pi Plus tensiometer (Kibron, UK). 1.5 ml of solution was placed into a sterile cup holder. Triplicate measurements were carried out at 20 °C.

For oil/water interfacial tension measurements 1% w/w NCM centrate fraction solutions were serially diluted to obtain 0.1%, 0.01%, 0.001% and 0.0001% w/w NCM

solutions. A sessile sunflower oil droplet was ejected from a 1.067 mm diameter needle at a rate of 400 µl/min into a glass sample cell containing the centrate fraction solution. The evolution of the oil droplet shape was captured over 60 min using a Krüss Easydrop tensiometer (Krüss GmbH, Germany). A 3000-frame video of the droplet was captured at a frame rate of 50 frames per second. The interfacial tension at the oil/water interface was calculated frame by frame using the associated Drop Shape Analysis software. Measurements were repeated four times. Retraction tests were performed on the aged droplet by removing oil from the droplet at a rate of 100 µl/min with visual observation of the resulting oil/water interface.

Confocal microscopy

Microscopic images of centrate fraction solutions, foams, oil-in-water emulsions and hydrogels were obtained using a Leica TCS2 confocal laser scanning microscope (Leica

Microsystems, Germany). Images were recorded at a resolution of 512 × 512 pixels and analysed using the associated DM SDK version 4.2.1 software.

For the imaging of solutions, foams and hydrogels 1% and 10% w/w NCM solutions of the centrate fractions were supplemented with the fluorescent dye Rhodamine B. The dye was excited at 514 nm, the collection range was 600–700 nm and a 10×/0.25 dry lens was used. Foams and hydrogels were prepared following the procedures described in the foaming properties and rheological properties sections.

The emulsions were prepared following the procedure described in the emulsifying properties section. Traces of Nile Red dye (Sigma Aldrich Co., UK) were added to the oil prior to mixing with the centrate fraction solution to stain the resulting emulsion oil droplets. The dye was excited at 549 nm and fluoresced light was collected at the emission maximum of 628 nm. A 63×/1.40–0.60 oil lens was used.

Statistical analysis

Statistical comparison of the data obtained with the different samples for a given test was carried using the SPSS Statistics 23.0 software (IBM, USA) with a one-way ANOVA test followed by a post hoc Tukey's HSD (honestly significant difference) test for pair-wise multiple comparison. A p value of 0.05 was used as cut-off for significance.

Table 1 Characterisation of centrate fractions

Fraction	Molecule range	Nitrogen-containing material (%) ($n=3$)	pH in aqueous solution
Centrate	n/a	47.3 ± 1.2	4.2
R100	> 100 kDa	56.7 ± 4.7	4.2
R100+5	$5 > \text{kDa} < 100$	69.8 ± 0.3	4.3
R100+50	$50 > \text{kDa} < 100$	69.2 ± 1.0	4.3
R100+50+5	$5 > \text{kDa} < 50$	71.6 ± 2.0	4.3

Human/animal rights

This article does not contain any studies with human or animal subjects.

Results and discussion

Centrate fraction characterisation

The rationale behind using the whole centrate stream for ultrafiltration instead of its centrifugation supernatant was based on an initial functional comparison between the two samples, during which the whole centrate showed higher foaming and emulsifying properties than its supernatant (results not shown). The pH of all the centrate fractions was more acidic (4.2–4.3) than the fermentation broth (6.0) due to the consumption of ammonia added as source of nitrogen for growth of the organism and as pH regulator (Table 1).

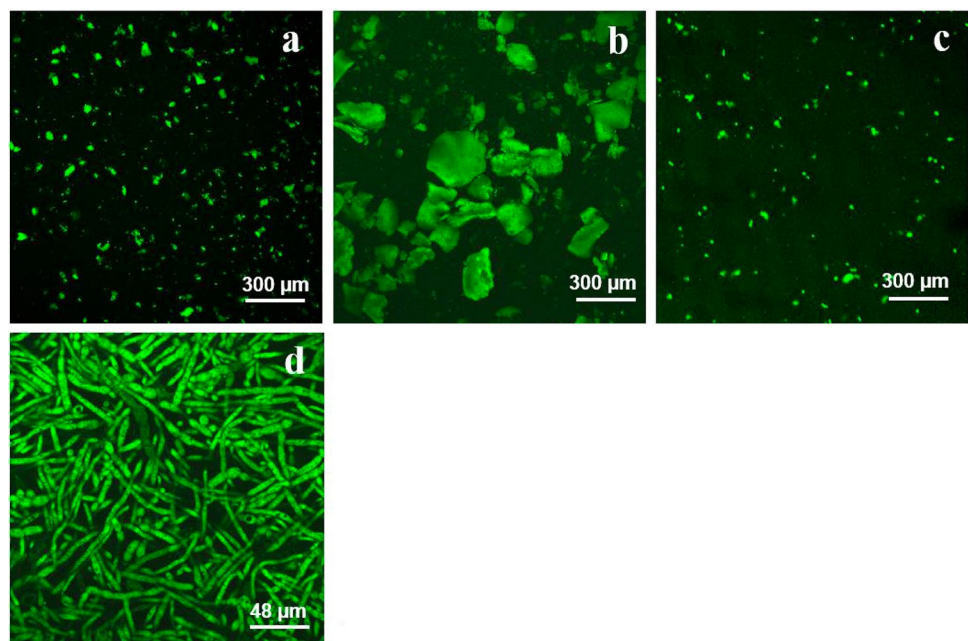
Fungal cell and mycelial debris were observed in the centrate and R100+5 solutions (Fig. 1a, c), with the

characteristic mycelial network of the Quorn fermentation broth centrifugation deposit chosen as reference (Fig. 1d). Much larger structures were present in R100 (Fig. 1b), resulting from the aggregation of the mycelial debris observed in the centrate during their retention on the 100 kDa ultrafiltration membrane. Fungal aggregate formation has been attributed to a combination of electrostatic interactions, hydrophobic interactions and specific interactions between cell wall components including proteins and polysaccharides [21] and the influence of temperature on mycelial aggregation was previously reported for the filamentous fungus *Rhizopus* sp. [22]. The aggregation process observed could thus have resulted from the pressure exerted on the ultrafiltration membrane-retained material and/or from the temperature increase occurring during ultrafiltration.

The successive ultrafiltration steps resulted in an increase in nitrogen-containing material (NCM): 47.3% (centrate), 56.7% (R100) then 69.8–71.6% (further retentates) (Table 1). Following the 100 kDa ultrafiltration step the retention of the aggregated mycelial debris in R100 (observed in Fig. 1b) concentrated nitrogen-containing cell wall and cell membrane constituents (including phospholipids, sterols, glycosphingolipids, sphingomyelins, chitin, chitosan and glycoproteins) and contributed to the NCM increase in this sample.

A fraction of the R100 sample did not migrate on the Native-PAGE gel (band g), indicating that material larger than the higher protein marker band size (200 kDa) was present (Fig. 2b). Faint bands g (corresponding to non-migrating material) were also reported on the Native-PAGE profiles of the centrate and Quorn fermentation broth centrifugation deposit. Concentrated and faint

Fig. 1 Confocal microscopy of centrate fractions (1% w/w NCM concentration, original pH, rhodamine, magnification $\times 10$ (a–c) or $\times 63$ (d)). **a** Centrate, **b** R100, **c** R100+5, **d** Quorn fermentation broth centrifugation deposit



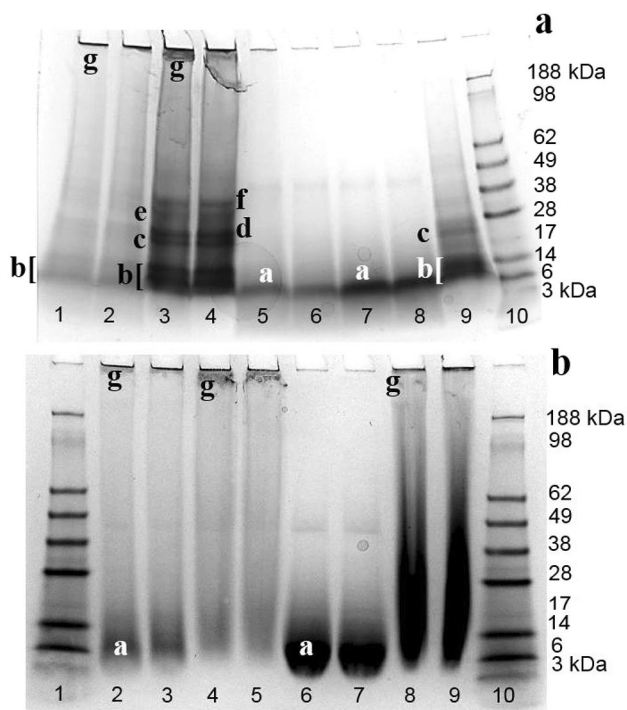


Fig. 2 SDS-PAGE (**a**) and Native-PAGE (**b**) of centrate and broth fractions (1% w/w NCM, original pH). **a** Centrate (lanes 1–2), R100 (3, 4), R100+50 (5, 6), R100+50+5 (7, 8), Quorn fermentation broth centrifugation deposit (9), See Blue reference marker (10). **b** See Blue marker (1), centrate (2, 3), R100 (4, 5), R100+50+5 (6, 7), Quorn fermentation broth centrifugation deposit (8, 9), See Blue reference marker (10)

bands g (non-migrating material) were also, respectively, observed on the SDS-PAGE profiles of R100 and centrate, however, several specific concentrated bands were also present for R100 below 100 kDa in the 10–15 kDa (band b), 20–30 kDa (c and d) and 30–40 kDa (e and f) regions (Fig. 2a). These results highlighted the presence of R100 protein aggregates in band g and their breakdown into oligomers or monomers (bands b to f) in the presence of SDS and β -mercaptoethanol. The electrophoretic profiles of R100 also indicated that, in addition to the mycelial aggregates, the concentration of protein aggregates composed of monomers and/or oligomers between 10 and 40 kDa in this fraction also contributed to the increase of NCM level following the 100 kDa ultrafiltration. The Native and SDS-PAGE profiles of the R100+5, R100+50 and R100+50+5 fractions proved similar, with a main band (a) observed below 10 kDa corresponding to protein monomers concentrated as a result of the successive ultrafiltration steps, which contributed to the further increase of NCM concentration in these samples.

Centrate fraction composition

173 proteins were successfully identified based on MOWSE scores of 85 or greater (5% probability of misidentification) and identification with more than one peptide, as defined by Pappin et al. [23]. Out of the 173 identified proteins, the presence of 30 ribosomal proteins and 6 heat-shock proteins (Hsp) resulted from the heat-shock RNA-reduction heating step. Appendix A in the supplementary material highlights the proteins reported in higher relative proportions in R100 in comparison with other centrate fractions. These included a cerato-platanin, HEX-1, the heat shock 70 kDa protein 4 and a number of elongation factors and tubulins. The higher proportions of a number of proteins in R100 were due to the presence of the large mycelial aggregates observed in Fig. 1b. In particular cerato-platanins have been reported within the cell wall of fungal hyphae and spores [10, 11] and members of the Hsp70 (heat-shock protein) family have been shown to be located in the cell wall of *Saccharomyces cerevisiae* [24] and *Candida albicans* [25].

A large number of proteins below 100 kDa were reported in the R100 fraction, and the majority of these proteins matched in terms of molecular mass with the concentrated bands (a to g) specifically observed on the SDS-PAGE profile of R100 (Fig. 2). Moreover several of these proteins have been characterised by their capacity to self-assemble, including cerato-platanins, HEX-1, translation elongation factors and tubulins, confirming the presence of protein aggregates in this fraction which were reduced to oligomers and monomers under the proteomic sample preparation or SDS-PAGE conditions. In particular cerato-platanins from *Trichoderma* are known to form dimers [26]. The cerato-platanin EPL1 from the fungus *Trichoderma atroviride* was reported to form ordered self-assembled layers at the air/water interface [9] and hydrophobic/hydrophilic interfaces [27]. The HEX-1 protein was also shown to self-assemble into three-dimensional lattices to form Woronin bodies, which are peroxisome-derived organelles that maintain cellular integrity and prevent cytoplasmic bleeding in response to hyphal wounding and cellular damage by sealing septal pores [28]. The heat-shock RNA-reduction process carried out on the Quorn fermentation process has been reported to induce such damage to fungal cells [5], resulting in the possible aggregation and concentration of HEX-1 in the large mycelial structures observed in R100.

Appendix B in the supplementary material lists the metabolites which were identified in centrate and previously reported in the literature for their functional properties. The presence of mycelial debris in the centrate and their aggregation and concentration in the R100 fraction (Fig. 1b) implied the presence of fungal cell membrane constituents (phospholipids, sterols, glycosphingolipids and sphingomyelins) and cell wall constituents (chitin,

chitosan, beta-glucans and glycoproteins). These materials could also have diffused out of the fungal cells through the damaged cell walls as a result of the RNA-reducing heat-shock process as previously reported [5]. Both α -*N*-acetylglucosamine, monomer unit of chitin and chitosan, and its derivative α -*N*-acetylglucosamine-6-phosphate were identified in centrate. Chitin, chitosan and their derivatives are used as functional ingredients in the food industry due to their foaming, emulsifying, thickening and gelling properties [13], including those of fungal origin [14]. A range of fungal cell membrane lipids were reported, including phospholipids, lyso phospholipids, sterols and sterol esters, glycosphingolipids and sphingomyelins. Phospholipids (lecithins) and lysophospholipids are used as emulsifiers [29] while phytosterols and phytosterol esters are known to form oleogels [30]. Gelling properties have been reported for several sphingolipid groups, including ceramides and sphingomyelins [31] and glycosphingolipids [32]. Two functional polysaccharides (inulin and a galactan) were identified. Inulin is used for its viscosifying and gelling properties [33] and was previously identified in the fungus *Aspergillus oryzae* KB [34]. Galactans are constituents of cell walls and used as viscosifying and gelling agents [35]. The production of galactans by fungi has previously been reported in the genus *Pleurotus* [36].

A range of nucleobases, nucleosides and nucleotides (including guanine-based compounds) and their derivatives were reported in the centrate metabolome. The presence of these compounds resulted from the breakdown of cellular RNA releasing nucleotides and the subsequent breakdown of these nucleotides into nucleosides and nucleobases as a result of the RNA-reducing heat-shock treatment. Viscosifying and gelling properties have been reported for the guanine nucleobase and for guanine-based nucleosides and nucleotides due to the ability of guanine to self-associate [15].

A number of monoglycerides and diglycerides and their derivatives, used as foaming and emulsifying ingredients [37], were identified as well as several glycosyldiglycerides, characterised by their foaming and emulsifying properties [38]. A range of triterpenoid and steroidal saponins were identified. These compounds have been characterised by their foaming and emulsifying properties [39] and several *Fusarium* strains were shown to produce saponins, including the triterpenoid saponin-producing *Fusarium avenaceum* [40] and *Fusarium* sp. PN8 [41]. Several fatty acyl glycosides, including rhamnolipids, were detected. Fungal rhamnolipids are used as foaming and emulsifying agents [42]. Several sugar alcohols, which are characterised by their viscosifying properties [43], were identified. A range of fatty amides including fatty acyl ethanolamines was detected. Foaming and emulsifying properties have previously been shown for this class of compounds [44].

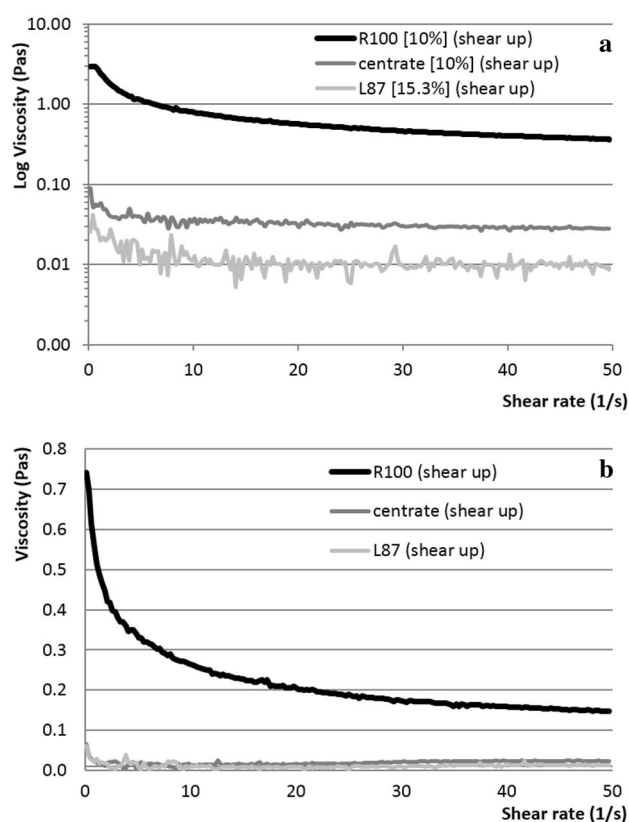


Fig. 3 Viscosity profiles of centrate fraction solutions (**a**) and centrate fraction emulsions (**b**) during shear sweep. **a** 10% w/w NCM concentration except 15.3% NCM w/w for L87, original pH, $n = 2$. **b** 5% w/w NCM concentration, original pH, $n = 3$

Rheological properties of centrate fractions

The functional profile of the R100 + 5 and R100 + 50 + 5 fractions proved very similar so not all the results obtained with R100 + 5 or R100 + 50 + 5 are shown. The yield obtained for the R100 + 50 sample was insufficient to test its functional profile. The final filtrate obtained (filtrate 100 + 50 + 5) did not prove functional (results not shown).

10% w/w NCM R100 solutions showed higher viscosities than similar solutions and emulsions prepared with L87 or other centrate fractions (Fig. 3a). The high viscosity reported in R100 solutions resulted from the presence of the large mycelial structures observed in Fig. 1b which resisted flow and from the presence of viscosifying compounds (including cell wall and membrane constituents such as chitin, chitosan and galactan). Similarly the high concentration of mycelial aggregates was previously correlated with a decrease of the flow index for fermentation broths of the filamentous fungus *Aspergillus terreus* [45]. 5% w/w NCM R100 emulsions also showed higher viscosities than similar emulsions prepared with L87 or other centrate fractions (Fig. 3b) due to the presence of fungal cells, mycelial debris and viscosifying

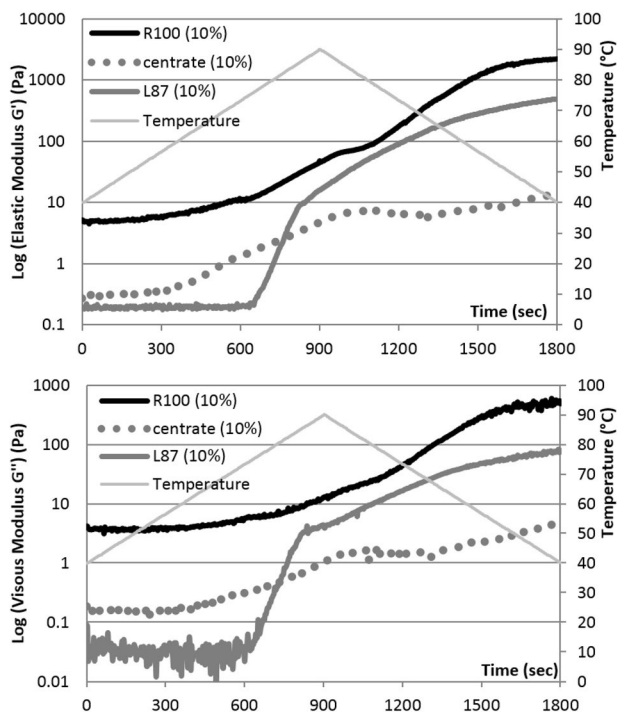


Fig. 4 Gelation profiles (elastic modulus G' and viscous modulus G'') of centrate fractions (10% w/w NCM concentration, original pH, $n=3$)

compounds released from the mycelial aggregates during emulsification.

Unheated 10% w/w NCM R100 solutions showed a higher viscoelasticity than those of L87 and other centrate fractions (Fig. 4), resulting from the presence of the mycelial aggregates observed in Fig. 1b. R100 displayed a gelation profile at 5% w/w NCM, whereas the centrate equivalent did not (results not shown). Both centrate and R100 fractions gelled at 10% w/w NCM while the R100 + 5 fraction did not gel at any of the NCM concentrations tested.

10% w/w NCM R100 hydrogels showed a very dense network (Fig. 5a) of entangled mycelial aggregates and filaments (Fig. 5b). The higher viscoelasticity reported for these gels in comparison with L87 and centrate ones (Fig. 4) was due to the presence of these structures and of gelling compounds (including cell wall and membrane constituents such as chitin, chitosan, galactan, phospholipids, sterols, glycosphingolipids and sphingomyelins). The entanglement of mycelial aggregates and filaments reported for R100 gels was reminiscent of the microstructure of Quorn products, which is responsible for their meat-like texture and described as a fibre gel composite composed of an entangled mass of mycoprotein hyphae with gelled albumen protein within the interstitial space [46]. The unique gelation of R100 at the lowest concentration tested (5% w/w NCM) was then due to its high concentration of gel-forming mycelial structures in comparison with the centrate which contained only a limited amount of mycelial debris and thus required a higher NCM concentration (10% w/w) to display a gel-like behaviour. In comparison, the gel obtained using L87 (Fig. 5c) showed a more open fractal-like gel network resulting in a lower viscoelasticity.

Foaming properties of centrate fractions

When collected following the 100 kDa filtration, the retentate 100 (R100) foamed strongly, which suggested a further concentration of surface-active material present in the centrate. Foams produced with 1% w/w NCM R100 solutions at the original pH (4.2) by gas-sparging (Fig. 6) proved more stable than L87 ones, whereas the other centrate fractions did not yield stable foams. Similarly the native R100 extract displayed a higher foam stability than other centrate fractions and L87 using the frothing assay (Fig. 7a). However, following frothing R100 showed a lower foaming ability than the other samples, in particular the R100 + 5 extract (Fig. 7a). The high foaming ability

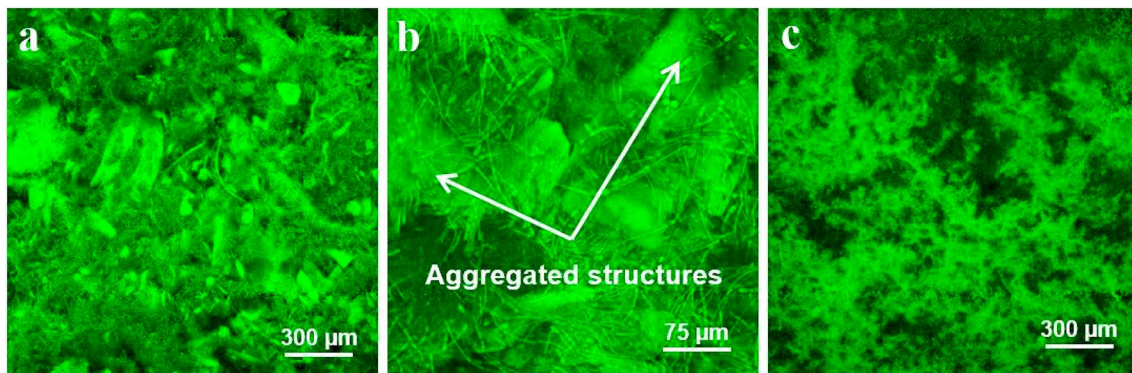


Fig. 5 Confocal microscopy of centrate fraction hydrogels (10% w/w NCM concentration, original pH, Rhodamine, magnification $\times 10$ (a, c) and $\times 40$ (b)). **a** R100, **b** R100, **c** L87

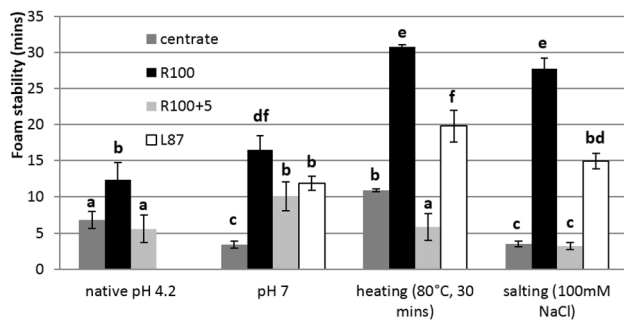


Fig. 6 Foam stability of the centrate (a, b) and broth (c) fractions as determined by the Rudin method (1% w/w NCM concentration, $n=4$). Different letters indicate statistically significant differences ($p < 0.05$)

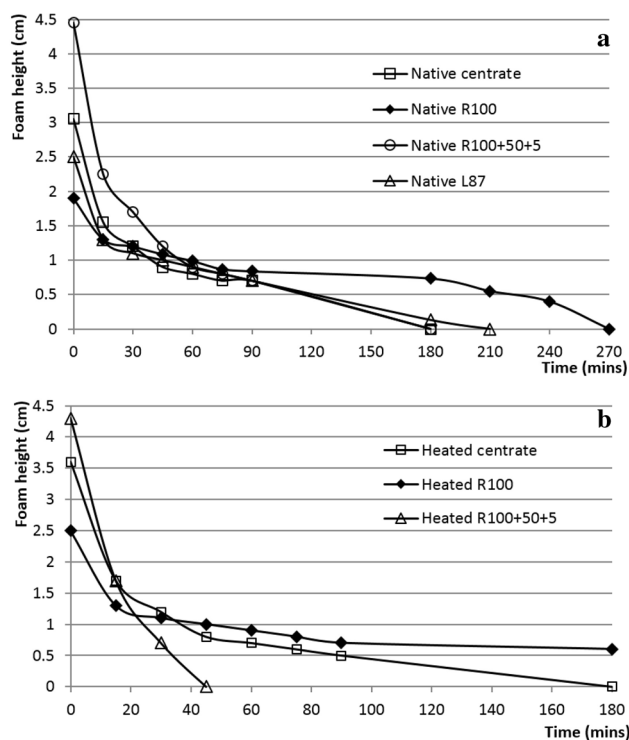


Fig. 7 Foaming ability and stability profiles of native (a) and heated (b) centrate fractions (1% w/w NCM concentration, frothing assay, original pH, 80 °C for 30 min, $n=3$)

measured for the centrate was in line with its ability to naturally foam in the centrifuge during processing of the Quorn fermented broth. Heat treatment applied prior to frothing improved the foaming ability of the R100 and centrate fractions, but did not change that of the R100+5 sample (Fig. 7b). Gas-sparging profiles showed that the foam stability of R100 was maintained when the pH was adjusted to 7 and was greatly enhanced following heating or in the presence of 100 mM NaCl (Fig. 6). R100

foams outperformed L87 ones in terms of stability in all conditions.

A high density of air bubbles was observed in centrate foams following frothing (Fig. 8a) while only few air bubbles were observed in R100 foams (Fig. 8b), which was in agreement with the low foaming ability of R100 (Fig. 7a). Micrographs showed that air bubbles in R100 foams were trapped in a dense network of mycelial and cell debris (Fig. 8c), which limited the number of air bubbles that could be entrapped thus explaining the low foaming ability of R100. Such mechanism was in agreement with previous findings highlighting that highly viscous fermentation media resulted in issues with gas–liquid mass transfer for the filamentous fungus *Aspergillus terreus* [45]. The high viscosity reported for R100 solutions (Fig. 3a) thus only allowed a limited number of air bubbles to be formed and transported within the liquid, leading to a poor foaming ability, but on the other hand prevented the destabilisation of the air bubbles formed by limiting their movement in the liquid, leading to a high foam stability.

Heating R100 solutions prior to foaming resulted in an increased foam stability following gas-sparging (Fig. 6), while in parallel an increased foaming ability but decreased foam stability were observed following frothing (Fig. 7b). Extrapolating from the micrographs obtained following heat-based gelation of 10% w/w NCM R100 solutions (Fig. 5b), heating the 1% w/w NCM R100 solutions should have resulted in an increased viscoelasticity and denser mycelial network. Such structure would have been maintained during the low-shear gas-sparging process, hence resulting in an enhanced entrapment and stabilisation of the air bubbles. On the other hand the high-shear frothing process would have partially disrupted the mycelial network, hence allowing for a higher number of air bubbles to be cavitated and transported but also limiting their stabilisation due to increased movement, thus leading to the increased foaming ability and decreased foam stability measured.

In parallel the centrate, R100 and R100+50+5 solutions showed significantly lower surface tension values than deionised water (72 mN/m) (Fig. 9). The surface tension of the R100 and R100+50+5 fraction solutions proved lower than that of L87 at 1% protein. R100 at 0.5%, 0.25%, and 0.1% still reduced the surface tension, equivalent to that obtained with a 1% L87 solution. These results highlighted the presence of molecules with surface activity at the air/water interface in the different centrate fractions.

The combined foaming, microscopy and tensiometry results suggested that small surface-active molecules concentrated in the R100+5 fraction were responsible for foaming ability, while specific material in the R100 fraction contributed to foam stability in addition to the physical stabilisation of air bubbles by the dense mycelial network. Foam-positive material specific to R100 included

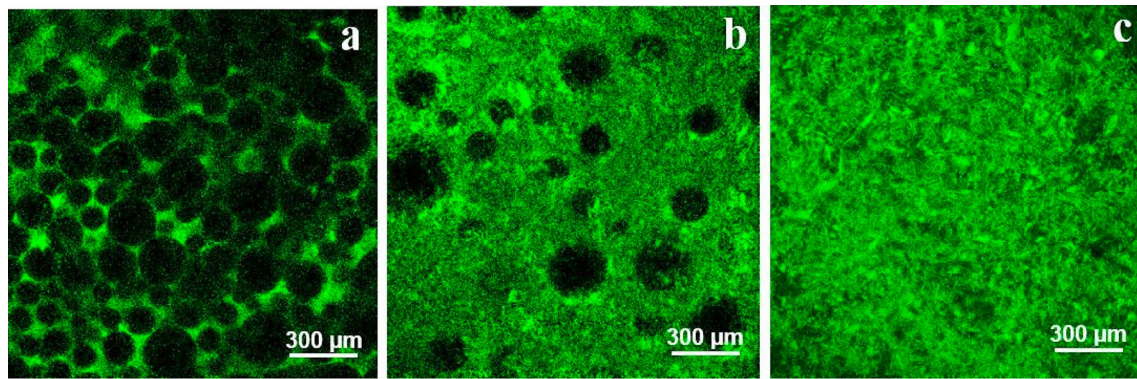


Fig. 8 Confocal microscopy of centrate fraction interfaces prepared by frothing (1% w/w NCM concentration, original pH, Rhodamine, magnification $\times 10$). **a** Air bubbles in centrate foam, **b** air bubbles in R100 foam, **c** mycelial structure in R100 foam

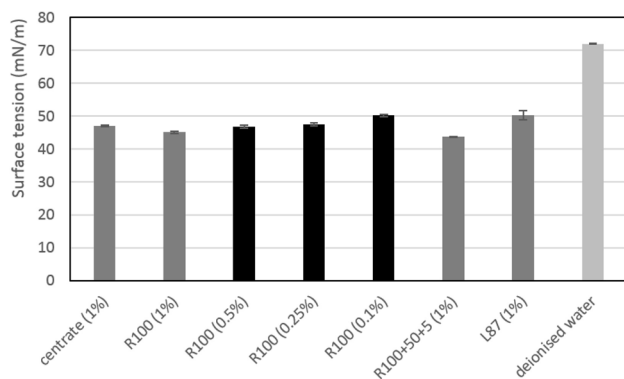


Fig. 9 Surface tension of centrate fractions (0.1–1% w/w NCM concentration, $n = 3$)

large mycelial aggregates, molecules larger than 100 kDa, foaming molecules and/or mycelial fragments or molecules released from mycelial aggregates during gas-sparging or frothing (including cell wall and membrane constituents exhibiting foaming properties such as chitin, chitosan and proteins). In particular the higher stability of R100 foams could be due to the concentration of the cerato-platanin in this fraction. Frischmann et al. [9] reported that solutions of cerato-platanin EPL1 from *Trichoderma atroviride* exhibited strong foaming properties. In addition, depending on their hydrophobicity the possible concentration of *Fusarium venenatum* cells and/or spores in the R100 fraction during ultrafiltration could also have contributed to the stabilisation of R100 foams as the shapes and sizes of bacterial cells, viruses and spores fall within the range suitable for Pickering stabilisation of biphasic dispersions including foams and emulsions [47]. Finally, a serpin (SERPB1) was identified in all centrate fractions. Steenbakkers et al. [48] previously reported a fungal serpin (celpin) from *Piromyces* spp. strain E2. Serpins Z4 and Z7 from barley have been characterised as foam-positive proteins in beer [49, 50].

The contribution of large mycelial aggregates was further supported by the higher foam stability obtained for the whole centrate (6.49 min, Fig. 6) in comparison with the centrate centrifugation supernatant (3.40 min, results not shown) in which they were absent. In addition the contribution of mycelial debris released from the breakdown of the large aggregates during frothing was further supported by the higher foam collapse time obtained for the whole centrate (180 min, Fig. 7) in comparison with the centrate centrifugation supernatant (50 min, results not shown) in which large aggregates were absent.

Emulsifying properties of centrate fractions

The centrate and R100 emulsions showed a comparable emulsifying activity index (EAI) to L87 at pH 4.2 and 7 (Fig. 10a). The EAI of R100 was greatly increased following prior heating and proved higher than that of L87. R100 emulsions showed a higher emulsifying stability index (ESI) than those of the other centrate fractions and L87 in all the conditions tested (Fig. 10b). The stability of R100 emulsions was greatly enhanced by either heating or adjusting the pH to 7. The whole centrate displayed higher EAI and ESI values (13.17 m^2/g and 19.72 min, Fig. 10) than the centrate centrifugation supernatant (5.89 m^2/g and 17.62 min, results not shown), highlighting the contribution of large mycelial aggregates to emulsifying properties.

Emulsions prepared with R100 at its original pH (4.2) displayed a smaller mean oil droplet size [D (3.2) surface weighted mean value of 8.8 μm] than L87 (16.1 μm at pH 7) and the other centrate fractions (10.4 μm for centrate and 16.5 μm for R100 + 5 at pH 4.2) (Fig. 11), which was in agreement with their higher EAI and ESI. Smaller oil droplet sizes were also observed for R100 emulsions in comparison with the other samples by confocal microscopy (Fig. 12). Small mycelial and cell debris were present in R100 emulsions (Fig. 12c), resulting from the breakdown of the large

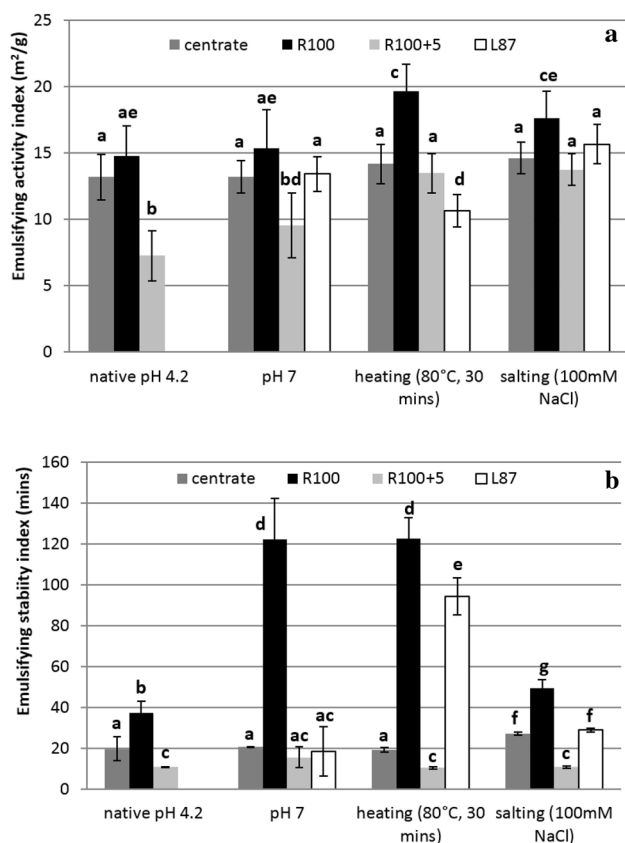
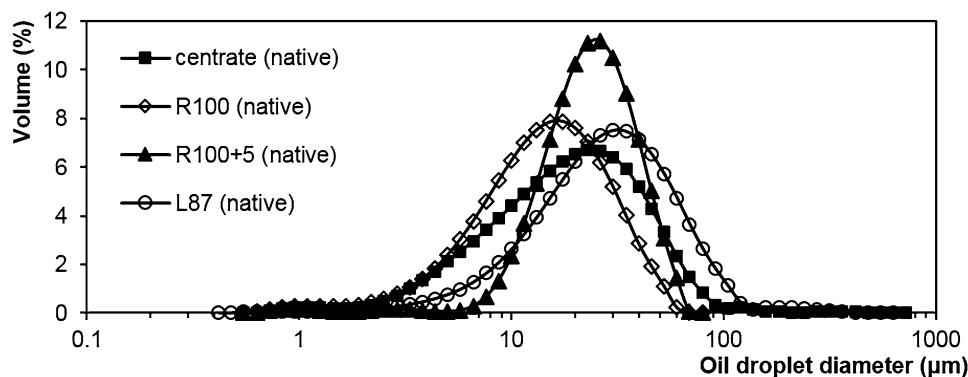


Fig. 10 Emulsifying ability (a) and stability (b) of the centrate and broth fractions as determined by the EAI/ESI method (1% w/w NCM concentration, $n=4$). Different letters indicate statistically significant differences ($p<0.05$)

structures observed in R100 solutions (Fig. 1b) during emulsification. Similarly to the stabilisation of R100 foams, the presence of mycelium fragments separated and limited the movement of oil droplets, contributing to emulsion stabilisation. The released mycelial fragments and the remaining mycelial aggregates also resulted in the enhanced viscosity reported for R100 emulsions (Fig. 3b), which further limited the movement of oil droplets and stabilised them.

Fig. 11 Oil droplet size distribution of emulsions stabilised with centrate and broth fractions (1% w/w NCM concentration, original pH, $n=3$)



Heating the R100 solutions prior to emulsification resulted in increased EAI and ESI (Fig. 10). Extrapolating from the micrographs obtained following heat-based gelation of 10% w/w NCM R100 solutions (Fig. 5b), heating the 1% w/w NCM R100 solutions should have resulted in a denser mycelial network. Such structure would have been partially disrupted during the high-shear emulsification process, releasing a number of mycelial fragments contributing to oil droplet formation and stabilisation, while the remaining denser network further stabilised the emulsion, thus leading to increased emulsifying ability and stability.

In parallel oil/water interfacial tension measurements were carried out. A wide range of dilutions (1–0.0001% w/w NCM) were screened. Based on the interfacial tension profiles obtained a 0.01% concentration was deemed optimal for comparison between samples. The interfacial tension of a sunflower oil droplet in water was used as control and measured at 32 mN/m. In the presence of 0.1% R100 or R100+5 the oil/water interfacial tension, respectively, decreased to 15 and 19 mN/m (Fig. 13). Following a 1-h ageing time the interfacial tension dropped to 11 and 14 mN/m, respectively. Although these decreases were not as pronounced as with 0.01% L87, these results confirmed the presence of surface-active moieties in the centrate fractions. Following a 1-h ageing process the drop surface crumpled or broke upon oil retraction (Fig. 14 and Table 2), indicating that the surface was covered with a rigid viscoelastic film that resisted deformation as the drop surface area was reduced. Oil droplets exhibited the strongest crumpling behaviour in R100 solutions and at an R100 concentration as low as 0.0001%. As the mycelial aggregates observed in Fig. 1b settled at the base of the cell over time and did not diffuse to the interface, these results confirmed the presence of interfacially active molecules in the centrate fractions and the concentration and/or specificity of some of this material in R100.

The combined EAI/ESI, oil droplet size, microscopy and tensiometry results highlighted the contribution of specific surface-active material (at the oil/water interface) and of viscosifying mycelium fragments (in the bulk emulsion) to the higher emulsifying properties measured for R100.

Fig. 12 Confocal microscopy of centrate, broth and whey protein emulsions (1% w/w NCM concentration, original pH, Nile Red, magnification $\times 63$). **a** Centrate, **b**, **c** R100, **d** R100+5, **e** L87

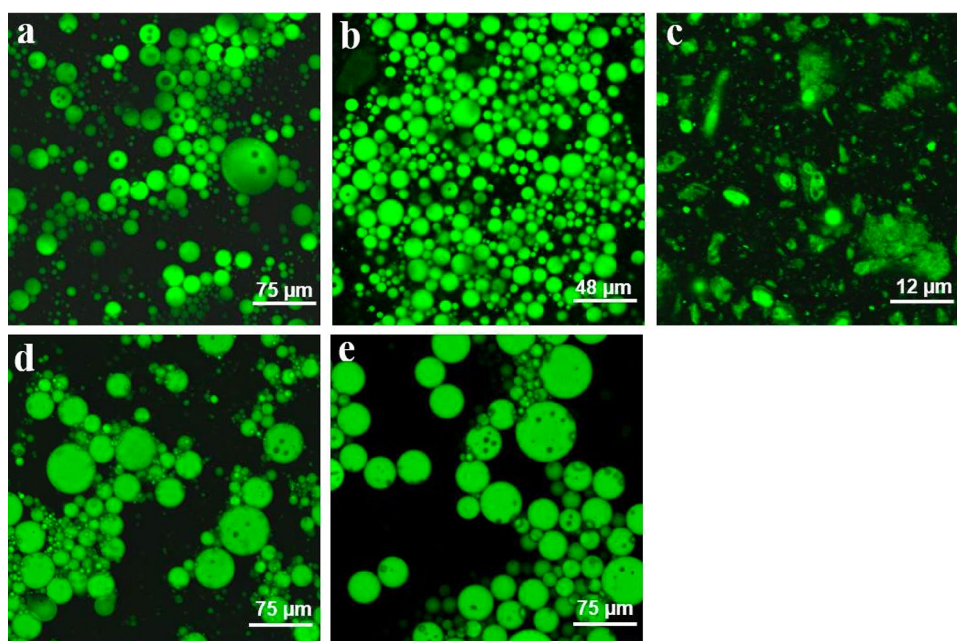


Fig. 13 Interfacial tension decrease at the oil/water interface in presence of dispersed centrate and broth fractions (oil droplet in 0.01% w/w NCM aqueous solution, original pH, $n=4$)

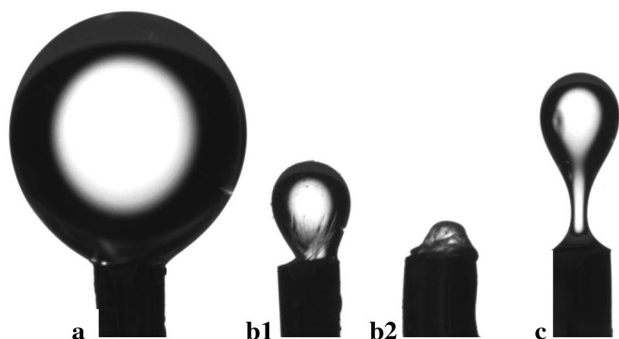
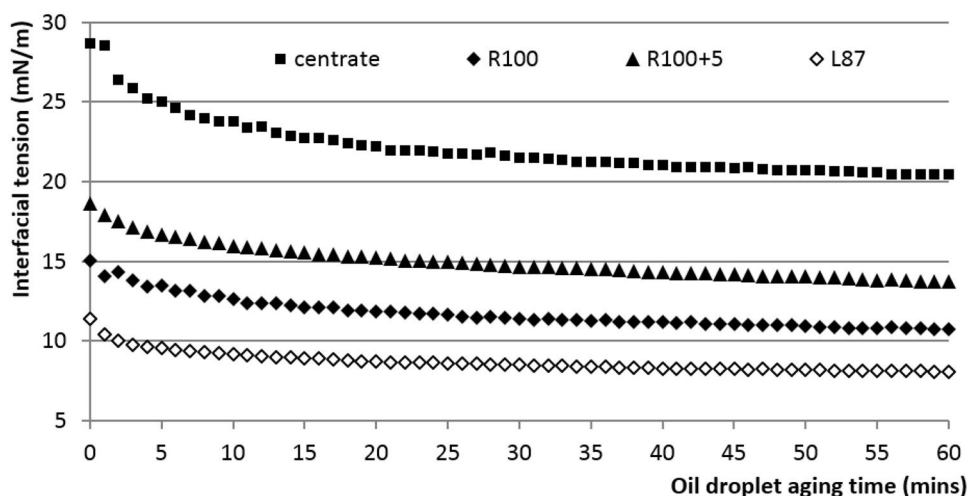


Fig. 14 Evolution of oil droplet shape during retraction after 1 h ageing in a 0.01% NCM R100 aqueous solution (original pH, $n=4$). (a) Full extension, (b1) crumpling during retraction after 1 h-ageing, (b2) further crumpling with further retraction, (c) droplet breaking during retraction after 1 h-ageing

Table 2 Oil droplet shape profiles upon retraction according to NCM concentration

	0.0001%	0.001%	0.01%	0.1%
Centrate	No crumpling	Crumpling ^a	Crumpling ^b	Crumpling ^b
R100	crumpling ^a	Crumpling ^b or breaking	Crumpling ^b or breaking	n/a (too turbid)
R100+5	No crumpling	Breaking	Crumpling ^b	Crumpling ^b

^aMinor crumpling observed

^bMajor crumpling observed

Emulsion-positive material included the released mycelial debris, molecular aggregates larger than 100 kDa, emulsifying molecules and/or molecules released from the mycelial

structures during emulsification (including cell wall and membrane constituents exhibiting emulsifying properties such as phospholipids, sterols, glycosphingolipids, sphingomyelins, chitin and chitosan). In addition the possible concentration of *Fusarium venenatum* cells and/or spores in R100 following ultrafiltration could have also contributed to the stabilisation of R100 emulsions. Dorobantu et al. [51] demonstrated that cells from four hydrocarbon-degrading bacteria species formed and stabilised oil-in-water and water-in-oil Pickering emulsions depending on their hydrophobicity. A partially hydrophobic moss spore (*Lycopodium clavatum*) also displayed the ability to stabilise oil-in-water emulsions [52, 53].

Conclusion

The proteomic and metabolomic profiling of the Quorn fermentation process co-product (centrate) coupled with the functional screening of a range of centrate-derived fractions confirmed the presence of functional material in this co-product. In particular the retentate 100 (R100) fraction, obtained following a 100 kDa ultrafiltration, displayed good foaming, emulsifying and rheological properties, highlighting the potential of functional extracts from the Quorn fermentation process as novel ingredients for the preparation of sustainable food products.

The study described the complex and specific nature of the R100's functional profile, with contributions reported for both mycelial structures and surface-active molecules. Large mycelial aggregates were observed in R100 solutions, contributing to their high viscoelasticity and high foam stability, and formed a fibre gel composite-type structure upon heating, resulting in highly viscoelastic R100 gels. In parallel tensiometry measurements showed the presence of surface-active moieties at the air/water and oil/water interfaces, highlighting the contribution of functional molecules (including cell membrane and cell wall constituents of the mycelial aggregates) and/or cell debris released from mycelial structures during foaming or emulsification to the high foaming and emulsifying properties of R100.

Additional studies are required to further understand the contribution of mycelial structures and surface-active molecules to these extracts. Future work will assess the possible applications of functional centrate extracts as novel sustainable ingredients for the food industry. Finally this study highlights the possibility to investigate the functional profile of the other Quorn fermentation process streams (fermentation broth and RNA-reduced broth).

Acknowledgements The authors wish to thank Dr Tim Finnigan, Dr Muyiwa Akintoye and Dr Sue Gordon from Marlow Foods for their support during this project.

Funding This work was supported by the Engineering and Physical Sciences Research Council (Grant number EP/J501682/1 Foaming and Fat Replacer Ingredients).

Compliance with ethical standards

Conflict of interest The authors declare that they have no conflict of interest.

Research involving human and/or animal rights This article does not contain any studies with human or animal subjects.

Open Access This article is distributed under the terms of the Creative Commons Attribution 4.0 International License (<http://creativecommons.org/licenses/by/4.0/>), which permits unrestricted use, distribution, and reproduction in any medium, provided you give appropriate credit to the original author(s) and the source, provide a link to the Creative Commons license, and indicate if changes were made.

References

- McMichael J, Powles C, Butler R (2007) Food, livestock production, energy, climate change, and health. *Lancet* 370:1253–1263
- Denny A, Aisbitt B, Lunn J (2008) Mycoprotein and health. *British. Nutr Bull* 33:298–310
- Edelman J, Fewell A, Solomons GL (1983) Myco-protein—a new food. *Nutr Abstr Rev Clin Nutr* 53:471–480
- Finnigan TJA, Lemon M, Allen B, Patton I (2010) Mycoprotein LCA and food 2030. *Asp Appl Biol* 102:81–90
- Ward PN (1996) A process for the reduction of nucleic acid content for a fungus imperfectus. WO Patent 95/23843
- Universal Protein Sequence. <http://www.uniprot.org/uniprot/>. Accessed 27 Feb 2019
- Wösten HAB, Bohlmann R, Eckerskorn C, Lottspeich F, Bolker M, Kahmann R (1996) A novel class of small amphipathic peptides affect aerial hyphal growth and surface hydrophobicity in *Ustilago maydis*. *EMBO J* 15:4274–4281
- Zapf MW, Theisen S, Rohde S, Rabenstein F, Vogel RF, Niessen L (2007) Characterization of AfpA, an alkaline foam protein from cultures of *Fusarium culmorum* and its identification in infected malt. *J Appl Microbiol* 103(1):36–52
- Frischmann A, Neudl S, Gaderer R, Bonazza K, Zach S, Gruber S, Spadiut O, Friedbacher G, Grothe H, Seidl-Seiboth V (2013) Self-assembly at air/water interfaces and carbohydrate binding properties of the small secreted protein EPL1 from the fungus *Trichoderma atroviride*. *J Biol Chem* 288:4278–4287
- Boddi S, Comparini C, Calamassi R, Pazzagli L, Cappugi G, Scala A (2004) Cerato-platanin protein is located in the cell walls of ascospores, conidia and hyphae of *Ceratocystis fimbriata* f. sp. *platani*. *FEMS Microbiol Lett* 233:341–346
- González-Fernández R, Aloria K, Valero-Galván J, Redondo I, Arizmendi JM, Jorrín-Novo JV (2014) Proteomic analysis of mycelium and secretome of different *Botrytis cinerea* wild-type strains. *J Proteom* 9:195–221
- Burkus Z, Temelli F (2005) Rheological properties of barley β -glucan. *Carbohydr Polym* 59:459–465
- Lapasin R, Stefancic S, Delben F (1996) Rheological properties of emulsions containing soluble chitosan. *Agro Food Ind High Tech* 7:12–17
- Quintela S, Villarán MC, López De Armentia I, Elejalde E (2012) Ochratoxin a removal from red wine by several oenological fining

- agents: bentonite, egg albumin, allergen-free adsorbents, chitin and chitosan. *Food Addit Contam Part A* 29(7):1168–1174
15. Peters GM, Davis JT (2016) Supramolecular gels made from nucleobase, nucleoside and nucleotide analogs. *Chem Soc Rev* 45:3188–3206
 16. Lynch JM, Barbano DM, Fleming JR (1998) Indirect and direct determination of the casein content of milk by Kjeldahl nitrogen analysis: collaborative study. *J AOAC Int* 81:763–774
 17. Le Bihan T, Martin SF, Chirnside ES, van Ooijen G, Barrios-Llerena ME, O'Neill JS, Shliaha PV, Kerr LE, Millar AJ (2011) Shotgun proteomic analysis of the unicellular alga *Ostreococcus tauri*. *J Proteom* 74:2060–2070
 18. Martin S, Munagapati VS, Salvo-Chirnside E, Kerr L, Le Bihan T (2012) Proteome turnover in the green alga *Ostreococcus tauri* by time course 15 N metabolic labeling mass spectrometry. *J Proteome Res* 11:476–486
 19. Rudin AD (1957) Measurement of the foam stability of beers. *J Inst Brew* 63(6):506–509
 20. Ogunwolu SO, Henshaw FO, Mock HP, Santos A (2009) Functional properties of protein concentrates and isolates produced from cashew (*Anacardium occidentale L.*) nut. *Food Chem* 115:852–858
 21. Zhang J, Zhang J (2016) The filamentous fungal pellet and forces driving its formation. *Crit Rev Biotechnol* 36(6):1066–1077
 22. Nyman J, Lacintra MJ, Westman JO, Berglin M, Lundin M, Lenartsson PR, Taherzadeh MJ (2013) Pellet formation of zygomycetes and immobilization of yeast. *New Biotechnol* 30(5):516–522
 23. Pappin DJ, Hojrup P, Bleasby AJ (1993) Rapid identification of proteins by peptide-mass fingerprinting. *Curr Biol* 3:327–332
 24. López-Ribot JL, Chaffin WL (1996) Members of the Hsp70 family of proteins in the cell wall of *Saccharomyces cerevisiae*. *J Bacteriol* 178(15):4724–4726
 25. López-Ribot JL, Alloush HM, Masten BJ, Chaffin WL (1996) Evidence for presence in the cell wall of *Candida albicans* of a protein related to the hsp70 family. *Infect Immunol* 64(8):3333–3340
 26. Vargas WA, Djonovic S, Sukno SA, Kenerley CM (2008) Dimerization controls the activity of fungal elicitors that trigger systemic resistance in plants. *J Biol Chem* 283:19804–19815
 27. Bonazza K, Gaderer R, Neudl S, Przylucka A, Allmaier G, Druzhinina IS, Grothe H, Friedbacher G, Seidl-Seiboth V (2015) The fungal cerato-platanin protein EPL1 forms highly ordered layers at hydrophobic/hydrophilic interfaces. *Soft Matter* 11(9):1723–1732
 28. Yuan P, Jedd G, Kumaran D, Swaminathan S, Shio H, Hewitt D, Chua NH, Swaminathan K (2003) A HEX-1 crystal lattice required for Woronin body function in *Neurospora crassa*. *Nat Struct Biol* 10(4):264–270
 29. Pichot R, Watson RL, Norton IT (2013) Phospholipids at the interface: current trends and challenges. *Int J Mol Sci* 14:11767–11794
 30. Matheson A, Dalkas G, Clegg PS, Euston SR (2018) Phytosterol-based edible oleogels: a novel way of replacing saturated fat in food. *Nutr Bull* 43(2):189–194
 31. Castro BM, de Almeida RF, Silva LC, Fedorov A, Prieto M (2007) Formation of ceramide/sphingomyelin gel domains in the presence of an unsaturated phospholipid: a quantitative multiprobe approach. *Biophys J* 93(5):1639–1650
 32. Westerlund B, Slotte JP (2009) How the molecular features of glycosphingolipids affect domain formation in fluid membranes. *Biochim Biophys Acta (BBA) Biomembr* 1788(1):194–201
 33. Mensink MA, Frijlink HW, van der Voort Maarschalk K, Hinrichs WLJ (2015) Inulin, a flexible oligosaccharide I: review of its physicochemical characteristics. *Carbohydr Polym* 130:405–419
 34. Kurakake M, Ogawa K, Sugie M, Takemura A, Sugiura K, Komaki T (2008) Two types of beta-fructofuranosidases from *Aspergillus oryzae* KB. *J Agric Food Chem* 56:591–596
 35. Delattre C, Fenoradosoa TA, Michaud P (2011) Galactans: an overview of their most important sourcing and applications as natural polysaccharides. *Braz Arch Biol Technol* 54(6):1075–1092
 36. Carbonero ER, Gracher AH, Rosa MC, Torri G, Sasaki GL, Gorin PA, Iacomini M (2008) Unusual partially 3-O-methylated alpha-galactan from mushrooms of the genus *Pleurotus*. *Phytochemistry* 69(1):252–257
 37. Moonen H, Bas H (2004) Mono- and diglycerides. In: Whitehurst RJ (ed) Emulsifiers in food technology. Blackwell Publishing Ltd, Oxford
 38. Keller RCA, Orsel R, Hamer RJ (1997) Competitive adsorption behaviour of wheat flour components and emulsifiers at an air-water interface. *J Cereal Sci* 25:175–183
 39. Kharkwal H, Panthari P, Pant MK, Kharkwal H, Kharkwal AC, Joshi DD (2012) Foaming glycosides: a review. *IOSR J Pharm* 2(5):23–28
 40. Wu H, Yang H, You X, Li Y (2012) Isolation and characterization of saponin-producing fungal endophytes from *Aralia elata* in Northeast China. *Int J Mol Sci* 13:16255–16266
 41. Jin Z, Gao L, Zhang L, Liu T, Yu F, Zhang Z, Guo Q, Wang B (2017) Antimicrobial activity of saponins produced by two novel endophytic fungi from *Panax notoginseng*. *Nat Prod Res* 31(22):2700–2703
 42. Al-Ahmad K (2015) The definition, preparation and application of rhamnolipids as biosurfactants. *Int J Nutr Food Sci* 4(6):613–623
 43. Zhu C, Ma Y, Zhou C (2010) Densities and viscosities of sugar alcohol aqueous solutions. *J Chem Eng Data* 55(9):3882–3885
 44. Xu W, Gu H, Zhu X, Zhong Y, Jiang L, Xu M, Song A, Hao J (2015) CO₂-controllable foaming and emulsification properties of the stearic acid soap systems. *Langmuir* 31(21):5758–5766
 45. Porcel EMR, Casas Lopez JL, Sanchez Perez JA, Fernandez Sevilla JM, Chisti Y (2005) Effects of pellet morphology on broth rheology in fermentations of *Aspergillus terreus*. *Biochem Eng J* 26:139–144
 46. Finnigan T (2011) Mycoprotein: origins, production and properties. In: Phillips GO, Williams PA (eds) Handbook of food proteins. Woodhead Publishing, Sawston
 47. Lam S, Velikov KP, Velev OD (2014) Pickering stabilization of foams and emulsions with particles of biological origin. *Curr Opin Colloid Interface Sci* 19(5):490–500
 48. Steenbakkens PJ, Irving JA, Harhangi HR, Swinkels WJ, Akhmanova A, Dijkerman R, Jetten MS, van der Drift C, Whistock JC, Op den Camp HJ (2008) A serpin in the cellulosome of the anaerobic fungus *Piromyces* sp. strain E2. *Mycological Research* 112(8):999–1006
 49. Li X, Jin Z, Gao F, Lu J, Cai G, Dong J, Yu J, Yang M (2014) Characterization of barley serpin Z7 that plays multiple roles in malt and beer. *J Agric Food Chem* 62(24):5643–5650
 50. Specker C, Niessen L, Vogel RF (2014) In vitro studies on the main beer protein Z4 of *Hordeum vulgare* concerning heat stability, protease inhibition and gushing. *J Inst Brew* 120:85–92
 51. Dorobantu LS, Yeung AKC, Foght JM, Gray MR (2004) Stabilization of oil-water emulsions by hydrophobic bacteria. *Appl Environ Microbiol* 70(10):6333–6336
 52. Binks BP, Clint JH, Mackenzie G, Simcock C, Whitby CP (2005) Naturally occurring spore particles at planar fluid interfaces and in emulsions. *Langmuir* 21(18):8161–8167
 53. Ballard N, Bon SAF (2011) Hybrid biological spores wrapped in a mesh composed of interpenetrating polymer nanoparticles as “patchy” pickering stabilizers. *Polym Chem* 2:823–827